

## SUPPLEMENTARY INFORMATION

# PHB green gels for the cleaning of paintings: new advances towards sustainable solutions

*S. Prati* <sup>\*[a]</sup>, *G. Sciutto* <sup>[a]</sup>, *F. Volpi* <sup>[a]</sup>, *C. Rehorn* <sup>[b]</sup>, *R. Vurro* <sup>[a,b]</sup>, *B. Bluemich* <sup>[b]</sup>, *L. Mazzocchetti* <sup>[c]</sup>, *L. Giorgini* <sup>[c]</sup>, *C. Samorì* <sup>[d]</sup>, *P. Galletti* <sup>[d]</sup>, *E. Tagliavini* <sup>[d]</sup>, *R. Mazzeo* <sup>[a]</sup>

**Figure S1:** Average molecular weights determined by GPC for different gel formulations and ageing times compared to that of the pristine PHB.

**Figure S2:** DSC scans, I (green) and II (blue) heating scans with the intermediate cooling (red), for PHB-EL and PHB-DMC gel formulations.

**Table S1:** Thermal properties of PHB based gels from DSC compared to pristine powder PHB.

**Figure S3:** Complex viscosity (A) and  $G'$  (full symbols) and  $G''$  (empty symbols) moduli (B) curves as a function of the sweep frequency for the two gel formulations.

**Figure S4:** Photomicrographs of cross sections sampled from a varnished area in visible (a) and UV light (b), from an area after treatment with EL by swabs in visible (c) and UV light (d); from an area after treatment with EL-PHB in visible (e) and UV light (f); from an area after treatment with DMC by swabs in visible (g) and UV light (h); and from an area after treatment with DMC-PHB in visible (i) and UV light (j).

**Figure S5:** Weight-weight percentage of the residual solvent in fragments collected from treated areas detected with SPME 1 hour and 24 hours after cleaning.

**Figure S6:** Comparison of two PHB-EL formulations. The lower concentration is described by two separate components that can be assigned to the binder and solvent (a). The higher concentration has broadened peaks and lower relaxation times are reached at later stages, suggesting embrittlement.

**Figure S7:** Portrait donated to the IPERION CH project (a). Photomicrograph of the cross section sampled before the cleaning treatments under: left: visible light; right: UV light (b). FTIR maps obtained in ATR mode (c).

**Figure S8:** Photomicrographs of cross sections sampled from areas after treatments with: EL by swabs: visible light (a), UV light (b); EL-PHB visible light (c), UV light (d); DMC by swabs visible light (e), UV light (f); DMC-PHB visible light (g), UV light (h).

**Figure S9:** Weight-weight percentage of the residual solvent in fragments collected from treated areas detected with SPME 24 hours after cleaning.

**Table S2:** Solvent-induced changes in the relaxation times of the binder.

## Supplementary information

The gelling conditions can affect the quality of the polymer [17], consequently the molecular weight was determined by GPC to assess the polymer stability upon processing. With both the two solvents, the polymer is well preserved and keeps its macromolecular integrity up to 11 weeks, as demonstrated in our tests (Figure S1), with just a slight reduction of the MW in the formulation containing EL. This confirms the possibility of storing the formulation once prepared. It can thus be made available as patches cut into any desirable size and shape to be used for restoration purposes.

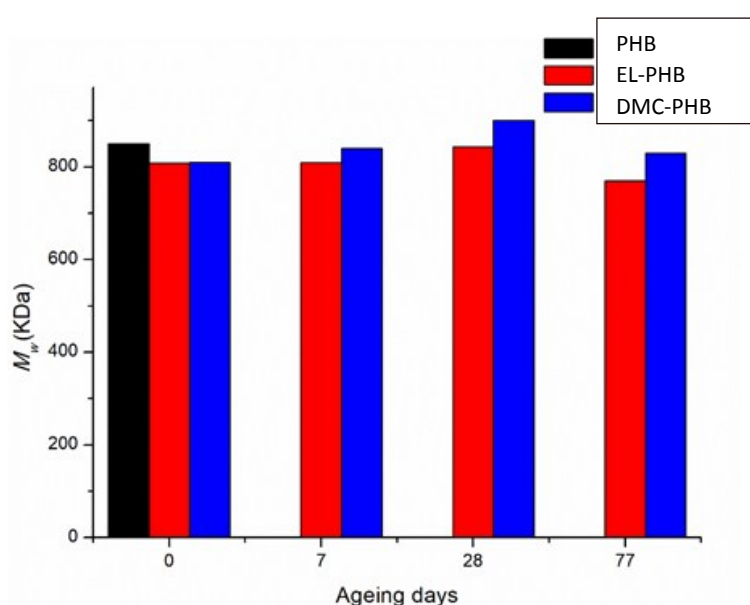


**Figure S1:** Average molecular weights determined by GPC for different gel formulations and ageing times compared to that of the pristine PHB.

The results of the DSC analysis of EL-PHB show only one endothermic transition in both the first and the second heating scans (Figure S2 and Table S1). According to previous results [17-18], this transition is due to the melting of the crystalline PHB phase in the gel, thus the signal observed in the second heating scan provides evidence of the thermo reversibility of the PHB gels. The melting temperature ( $T_m$ ) was slightly dependent on the solvent used. In fact, the  $T_m$  of the PHB-DMC gel was lower than that of the pristine polymer and of the previously discussed GVL [17] gel, although the overall crystal fraction was higher than

similar gels as well as pristine PHB. This suggests the formation of smaller and less perfect crystals that are more densely nucleated.

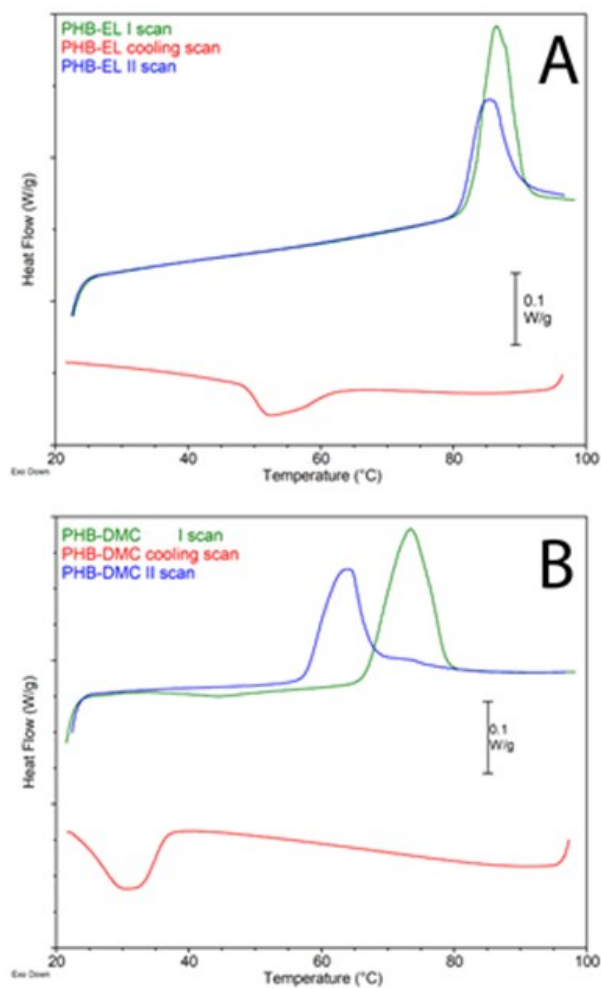


**Figure S2:** DSC scans, I (green) and II (blue) heating scans with the intermediate cooling (red), for PHB-EL and PHB-DMC gel formulations.

Sample	PHB (%wt)	1st scan			2nd scan		
		$T_m$ (° C)	$\Delta H_m$ (J/g)	$\chi C^a$ (%)	$T_m$ (° C)	$\Delta H_m$ (J/g)	$\chi C^a$ (%)
PHB	100	173	99.6	68.2	172	91.1	64
PHB-EL	7	89	7.8	78.7	88	6.3	63.3
PHB-	9	76	10.2	81.7	64	7.5	60.1

DMC							
-----	--	--	--	--	--	--	--

**Table S1:** Thermal properties of PHB based gels from DSC compared to pristine powder PHB.

a)  $\chi_c = \Delta H_{\text{PHB}} / \Delta H_{0\text{PHB}} * 100$ , where  $\Delta H_{\text{PHB}} = \Delta H / \%wt\text{PHB} * 100$ , and  $\Delta H_{0\text{PHB}}$  is 146 J/g the melting enthalpy for a theoretical 100% crystalline PHB [30].

According to rheological data (Figure S3), frequency sweeps of the PHB-EL and PHB-DMC materials indicate that stiff gels were formed. However, the gels can be cut without crumbling, so that they can be easily handled and applied on the surface of the painting.

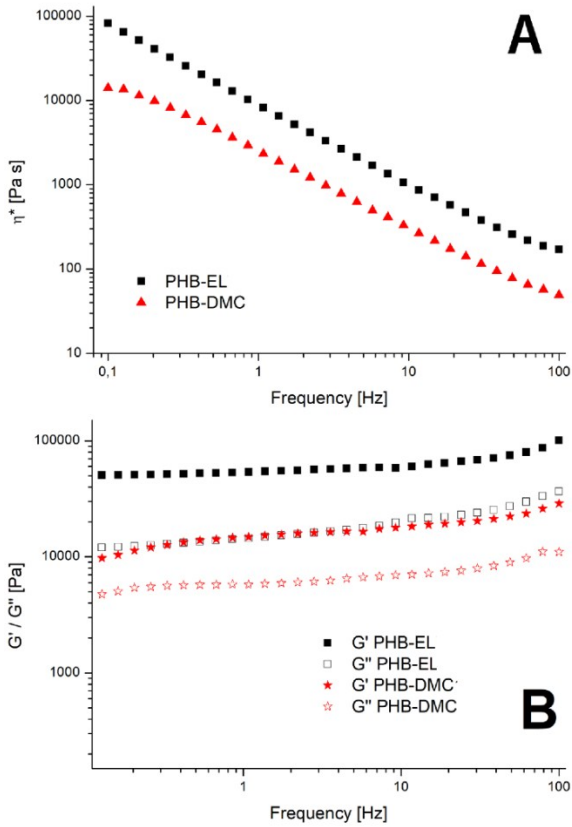


**Figure S3:** Complex viscosity (A) and  $G'$  (full symbols) and  $G''$  (empty symbols) moduli (B) curves as a function of the sweep frequency for the two gel formulations.

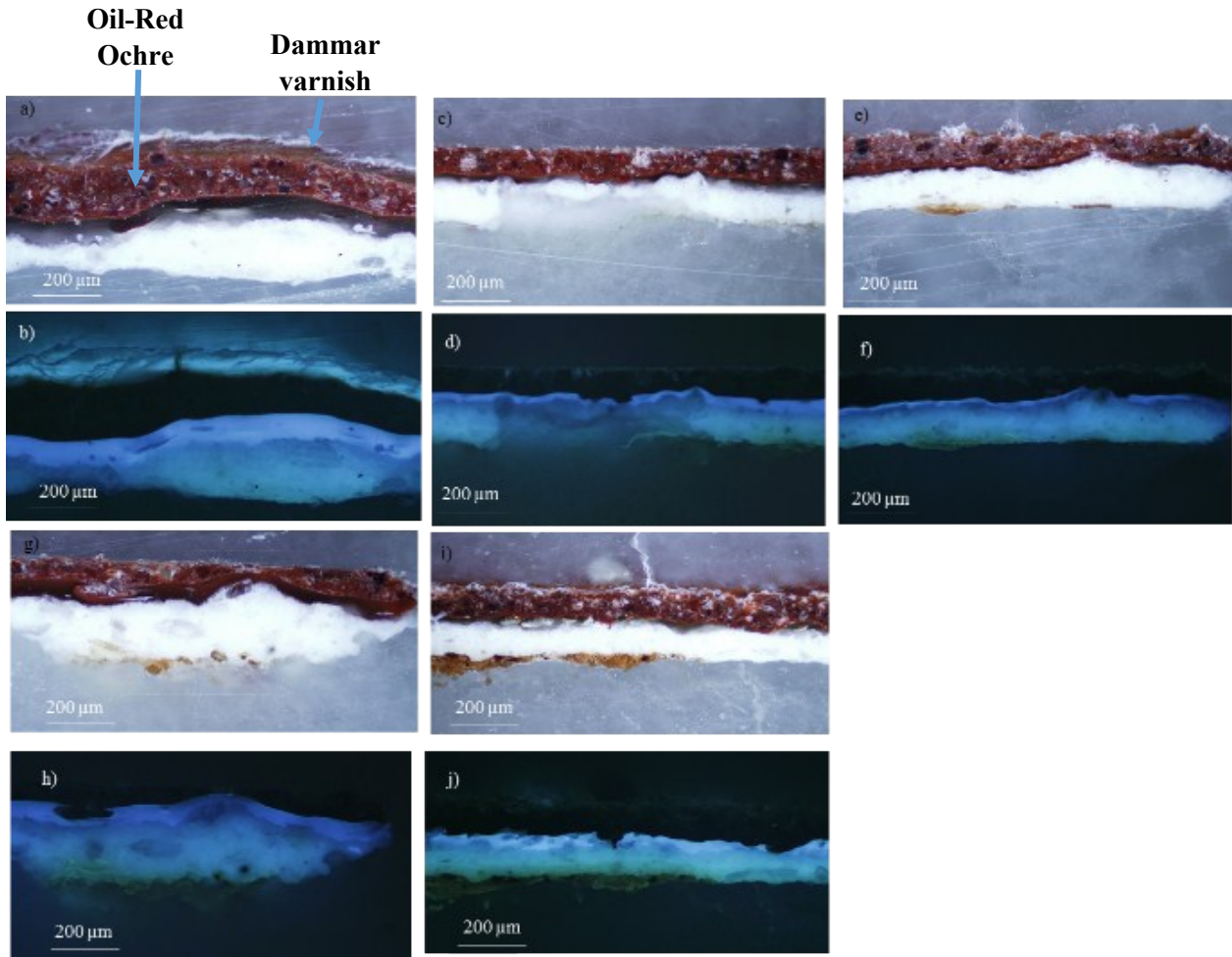


**Figure S4:** Photomicrographs of cross sections sampled from a varnished area in visible (a) and UV light (b), from an area after treatment with EL by swabs in visible (c) and UV light (d); from an area after treatment with EL-PHB in visible (e) and UV light (f); from an area after treatment with DMC by swabs in visible (g) and UV light (h); and from an area after treatment with DMC-PHB in visible (i) and UV light (j).

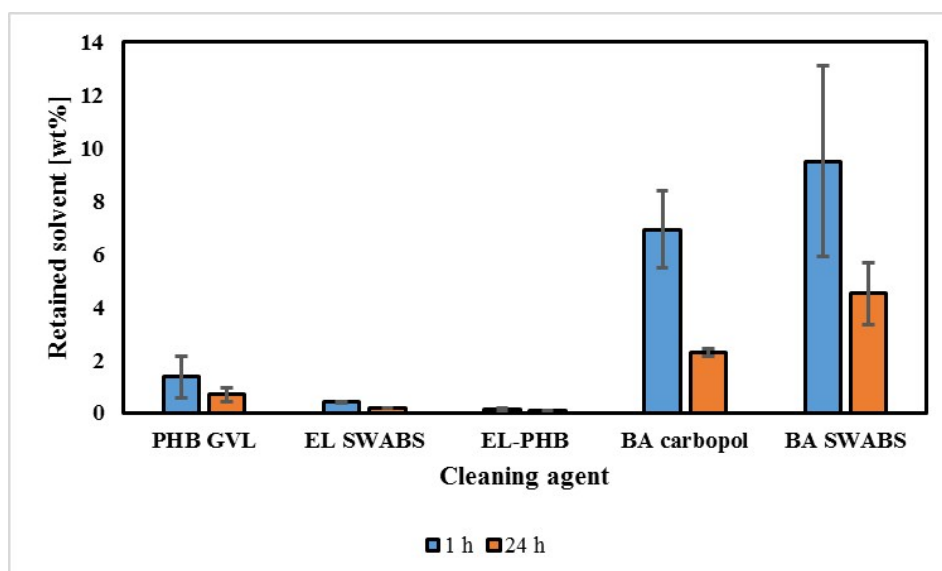


**Figure S5:** Weight-weight percentage of the residual solvent in fragments collected from treated areas detected with SPME 1 hour and 24 hours after cleaning.

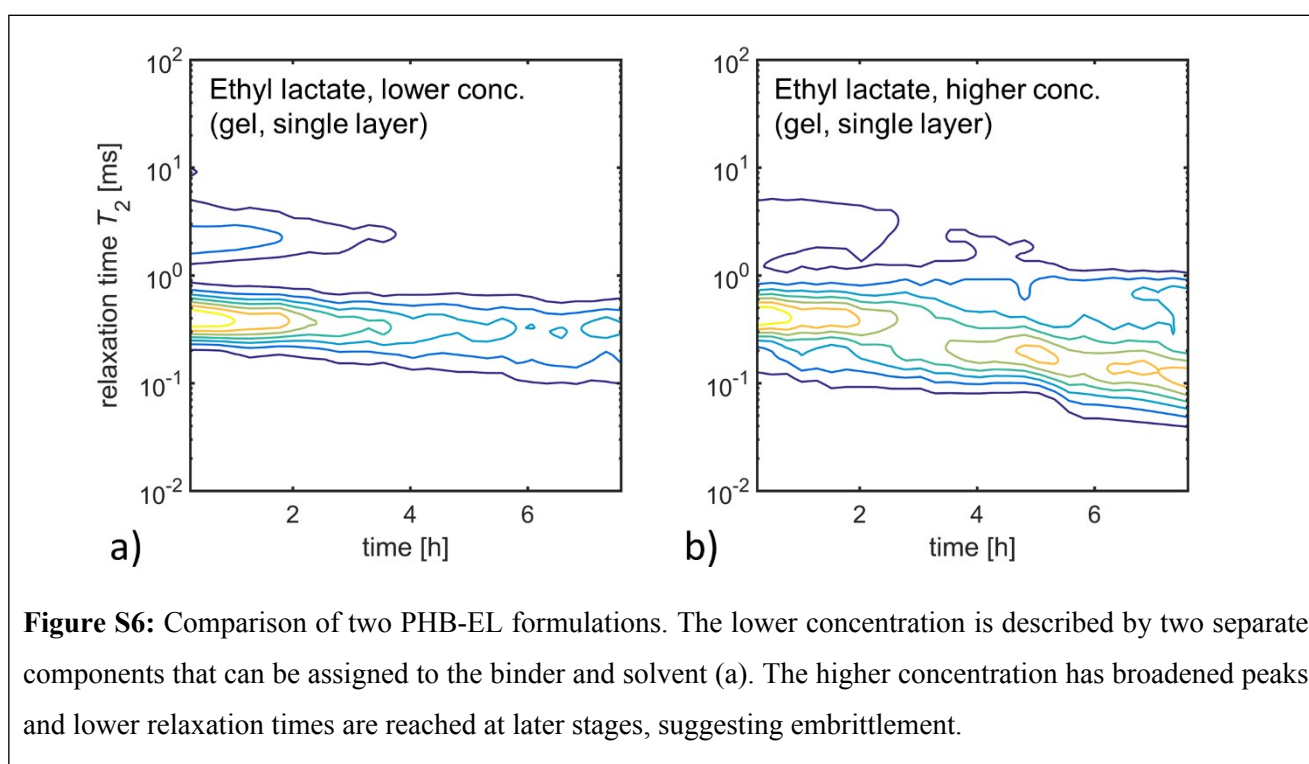


**Figure S6:** Comparison of two PHB-EL formulations. The lower concentration is described by two separate components that can be assigned to the binder and solvent (a). The higher concentration has broadened peaks and lower relaxation times are reached at later stages, suggesting embrittlement.

The concentration of a solvent within a gel is a parameter that is easily controlled in gels during their synthesis. In the traditional method the mass transfer can only be controlled manually by the conservator by applying the swab more quickly or by diluting the solvent with other liquids. The former may not always be viable, while in the latter the additional liquids may further modify the evaporation behaviour of the actual solvent.

In Section 3.2.2 we illustrate that this reduced mass transfer in gels compared to pure solvents can drastically limit the changes induced in the binder. We monitored the relaxation times during the first few hours after application. A direct comparison of two formulations of ethyl lactate gels substantiates the claim that not

only the type of solvent, but also the choice of its concentration is important when selecting a suitable candidate for cleaning. We compared a mixture of 13.3 ml EL per g PHB and one with only half the amount of solvent. Both gels were employed to clean varnished mock-ups and CPMG scans were performed on the binder layer for around eight hours, monitoring the immediate changes as well as the slow drying process of the EL (Fig. S6).

The relaxation time distributions of the two gels showed some resemblances, but the peaks were narrow in the case of the lower concentration. While there was an initial softening effect, the drying process showed a more embrittled structure at high solvent concentrations. The relaxation time components of the paint and binder are furthermore separate when less solvent was transferred, suggesting a reduced interaction of the two phases. Our results showed that the possibility of reliably controlling the solvent transfer is extremely valuable for researchers and conservators. The paper reports just the results of the more concentrated EL-PHB formulation because it was more effective in the removal of the varnish layer, showing similar results in terms of adsorbed solvent in the painting layer.



**Figure S7:** Portrait donated to the IPERION CH project (a). Photomicrograph of the cross section sampled before the cleaning treatments under: left: visible light; right: UV light (b). FTIR maps obtained in ATR mode (c).

The stratigraphy of a sample before the treatment comprises an external 15  $\mu\text{m}$  thick varnish layer (layer 2), a paint layer of about 10  $\mu\text{m}$  (layer 1) and a ground layer (layer 0).  $\mu\text{ATR}$  analyses (Figure S7c) showed that the coating layer is made of a terpenic varnish (1710  $\text{cm}^{-1}$  associated with the C=O stretching vibration of the carboxylic functions). The paint layer contains calcium oxalate (1315  $\text{cm}^{-1}$  assigned to the symmetrical

stretching of C-O), silicates (1100-1060  $\text{cm}^{-1}$  assigned to Si-O-Si stretching vibration) and a lipidic binder (1736  $\text{cm}^{-1}$ , assigned to the stretching of the C=O esters). The ground layer is composed of calcium carbonate, lead white (1400  $\text{cm}^{-1}$  and 837  $\text{cm}^{-1}$ ) and a lipidic binder.

The PHB-based green gels were applied for five minutes and their efficacy was compared to that of applying the same solvents with swabs. Furthermore, tests with benzyl alcohol applied with swabs were executed for comparison. The cross section of the painting sample collected from the surface before cleaning is reported in S8b together with the results of its characterisation with FTIR microscopy.

As observed in Figures S7b and S8, the thickness of the resin decreased after the treatments, though some residues were still detected. The two gels performed better than the swabs, leaving a mostly homogeneous surface.

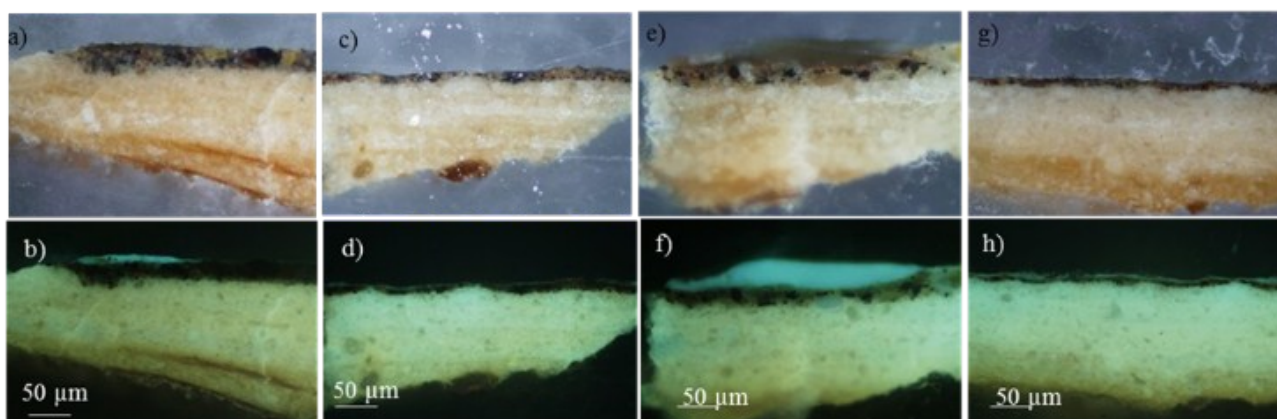
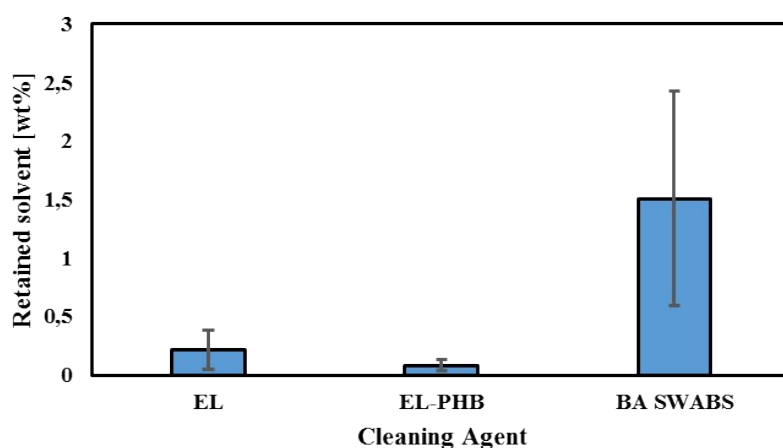


**Figure S8:** Photomicrographs of cross sections sampled from areas after treatments with: EL by swabs: visible light (a), UV light (b); EL-PHB visible light (c), UV light (d); DMC by swabs visible light (e), UV light (f); DMC-PHB visible light (g), UV light (h).

DMC gel resulted more effective than the same solvent applied with swabs. Indeed in the gelled form the contact time between the solvent and the varnish is increased. In fact, since the solvent is very volatile, the swabs tended to dry very quickly.

To limit the number of samples, retention studies with SPME were performed just 24 hours after cleaning (Figure S9). As previously observed on mock-up samples, the use of PHB-gels facilitated a more controlled release of the solvent and thus reduced the risk of retention. DMC residues were not present on the samples either when the gel was used or when the cleaning was performed with swabs. On the other hand, small



amounts of EL were detected with a lower content than retained when benzyl alcohol is employed.

**Figure S9:** Weight-weight percentage of the residual solvent in fragments collected from treated areas detected with SPME 24 hours after cleaning.

Treated and untreated areas were also analysed with the NMR-MOUSE. These experiments require far less time than our studies on the mock-up samples, yet they provide a simple answer to the underlying question as to whether there was lasting embrittlement caused by the cleaning. The reduction in the transverse relaxation time was thus analysed. The initial and resulting states of the sample points were compared by

calculating the relaxation times  $T_{2,b}$  and  $T_{2,a}$  before and after cleaning as  $\frac{T_{2,b} - T_{2,a}}{T_{2,b}}$  (Table S2). The

experiment was performed twice in separate spots to reduce the measurement error and to ascertain the

**Table S2:** Solvent-induced changes in the relaxation times of the binder.

Cleaning Agent	$T_2$ [ $\mu\text{s}$ ]		$\frac{T_{2,b} - T_{2,a}}{T_{2,b}}$
	$T_2$ [ $\mu\text{s}$ ] (prior)	(after cleaning)	
EL-PHB	150	110	26%
EL-PHB 2	149	117	26%
DMC-PHB	135	114	15%
DMC-PHB2	134	119	11%

